AD-A024 762

RIA-76-U307

AD

FA-TR-75075

A024762

REFLECTIVE DIELECTRIC COATINGS AS LASER COUNTERMEASURES

USADACS Technical Library
5 0712 01014394 8

TECHNICAL LIBRARY

October 1975

Approved for public release; distribution unlimited.

Pitman-Dunn Laboratory

U.S. ARMY ARMAMENT COMMAND
FRANKFORD ARSENAL
PHILADELPHIA, PENNSYLVANIA 19137

BEST AVAILABLE COPY

DISPOSITION INSTRUCTIONS

Destroy this report when it is no longer needed. Do not return it to the originator.

The findings in this report are not to be construed as an official Department of the Army position unless so designated by other authorized documents.

UNCLASSIFIED

SECURITY CLASSIFICATION OF THIS PAGE (When Data Entered)

REPORT DOCUMENTATION PAGE		READ INSTRUCTIONS BEFORE COMPLETING FORM
1. REPORT NUMBER FA-TR-75075	2. GOVT ACCESSION NO.	3. RECIPIENT'S CATALOG NUMBER
4. TITLE (and Subtitle) REFLECTIVE DIELECTRIC COATINGS AS LASER COUNTERMEASURES		5. TYPE OF REPORT & PERIOD COVERED Technical Research Report 6. PERFORMING ORG. REPORT NUMBER FA-TR-75075, October 1975
7. AUTHOR(s) JAMES W. DE VOCHT		8. CONTRACT OR GRANT NUMBER(s)
9. PERFORMING ORGANIZATION NAME AND ADDRESS FRANKFORD ARSENAL ATTN: PDS-A PHILADELPHIA, PA 19137		10. PROGRAM ELEMENT, PROJECT, TASK AREA & WORK UNIT NUMBERS AMCMS: 691100.11.84500.01 DA PROJ: 1T161102A31C
11. CONTROLLING OFFICE NAME AND ADDRESS USA ECOM FT. MONMOUTH NJ 07703		12. REPORT DATE October 1975 13. NUMBER OF PAGES 26
14. MONITORING AGENCY NAME & ADDRESS(if different from Controlling Office)		15. SECURITY CLASS. (of this report) UNCLASSIFIED 15a. DECLASSIFICATION/DOWNGRADING SCHEDULE N/A

16. DISTRIBUTION STATEMENT (of this Report)

Approved for public release; distribution unlimited.

17. DISTRIBUTION STATEMENT (of the abstract entered in Block 20, if different from Report)

18. SUPPLEMENTARY NOTES

19. KEY WORDS (Continue on reverse side if necessary and identify by block number)

Laser Countermeasures	Sensor Protection
Dielectric Reflector	Eye Protection
Dielectric Stack	Eye Safety
Dielectric Protection	

20. ABSTRACT (Continue on reverse side if necessary and identify by block number)

Two dielectric reflectors were evaluated. The computer model predictions of the transmission spectra for these reflectors closely reproduced the experimental optical density vs wave-length data for both planes of polarization and for various angles of incidence. The dielectric film designed for use at 1060nm vs neodymium lasers affords good protection against laser radiation up to 70 MW/cm^2 with luminous transmittance above 90% in the

DD FORM 1 JAN 73 1473 EDITION OF 1 NOV 65 IS OBSOLETE

UNCLASSIFIED

SECURITY CLASSIFICATION OF THIS PAGE (When Data Entered)

20. ABSTRACT: (Cont'd)

visible region. Optical densities were also measured as a function of angles of incidence of the laser beam on this film. The optical density decreased from about 4.0 to about 3.5 as the angle of incidence increased from normal to about 30°.

A second reflector was designed to reject both 1060nm and 530nm radiation. This filter exhibited an OD of 2.0 at both 1060 and 530nm. The optical density remained approximately constant for angular deviations to about 40° from the normal at power densities up to 65MW/cm^2; however, the luminous transmittace was only about 7%. Both of these dielectric devices showed good resistance to damage by high power density Q-switched Nd and 2xNd pulses.

TABLE OF CONTENTS

List of Illustrations

List of Illustrations (Cont'd)

INTRODUCTION

There are several types of military lasers currently in use which emit pulsed neodymium (Nd) and, potentially, doubled Nd light. The accepted maximum values at the cornea for safe eye exposure to these lasers are about 10^{-7} J/cm^2, (See Reference 1). In order to meet these eye safety requirements laser attenuation is required which strongly rejects or absorbs the threat radiation (optical density of 5 to 6). Similar protection is required for various types of seeking devices presently employed by guided missiles which use intensifying optics.[2]

Previous objections to the use of dielectric coatings to reflect or attenuate laser radiation include: (a) the high cost of production, (b) poor weatherability, and (c) severe angular dependency of reflectivity. Recent technological advances in control and measurement of thicknesses of vapor deposited or sputtered coatings have considerably reduced the uncertainties in preparation of multiple layers with predetermined thicknesses resulting in a lower cost per acceptable copy. Poor weatherability and abrasion resistance may be overcome by careful design of the optical path to accommodate the rejection filters in a protected enclosure, or by the use of protective coatings, while the angular dependency of the reflectivity can be offset by designing a thin film stack which has adequate reflectivity over the desired range of angles.

This report describes the evaluation of two thin film stacks fabricated by outside contractors. One selectively reflects at 1060 nm and transmits elsewhere, while the other reflects at both 1060 nm and 530 nm. The optical designs of the two reflectors were used in our computer programs to calculate optical density as a function of wavelength and angle of incidence. In both cases the experimental reflectivities were found to agree quite well with the computer predictions.

---

1 "Control of Hazards to Health from Laser Radiation," Dept. of the Army Technical Bulletin TB MED 279, 18 September 1974.

2 "E-O Sensor Susceptibility to Laser Radiation," J.R. Anderson, L. Esterowitz, and D.L. Weinberg, NRL, The Proceedings of the 1973 DoD Laser Effects/Hardening Conference, ed. N.F. Harmon, The Mitre Corp., M73-115, April 1974, Vol. 1, p. 117; "Permament Laser Damage Thresholds of IR Detectors," L. Esterowitz, F.J. Bartoli, M.R. Kruer, and R.E. Allen, NRL Report #7867, 12 May 1975.

EXPERIMENTAL*

Sample LE[3] conformed to the optical design shown in Figure 1.

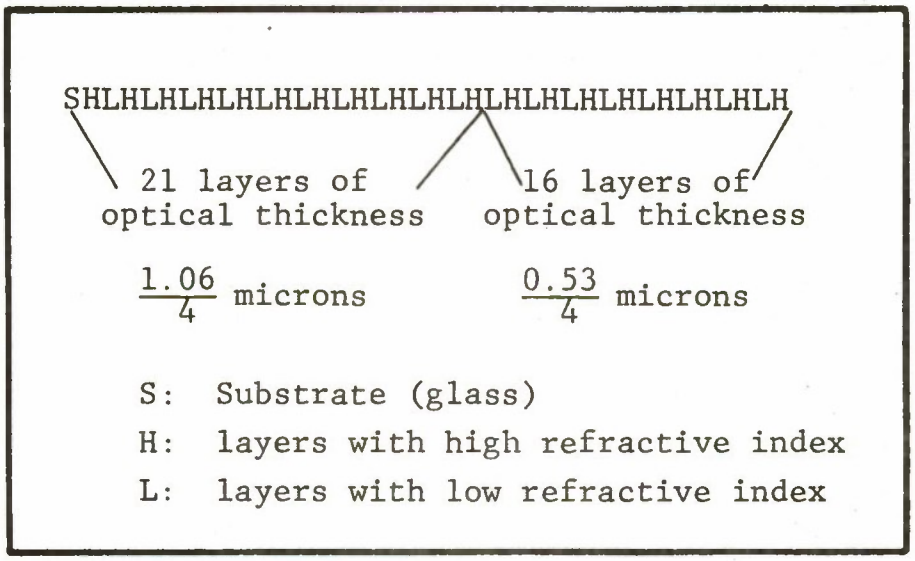

Figure 1. Optical Design of Specimen LE

Three different types of plastics, polycarbonate (Lexan), cellulose propionate, and polymethyl methacrylate, as well as glass had been tried as substrates by the contractor. All of the plastics either warped severely or the coatings failed to adhere well to them. Glass, however, turned out to be a very suitable substrate and was the only one used in this study.

The optical design of sample VP[4] is shown in Figure 2. Further details concerning the fabrication process or the materials were not available.

---

* References to manufacturers and fabricators of equipment and specimens in this report merely reflect the judgment of the author and in no way are to be taken as an endorsement by the United States government.

3 This sample was supplied by Laser Energy, Inc., Rochester, NY.

4 This sample was supplied by the Valpey Corp., Holliston, MA.

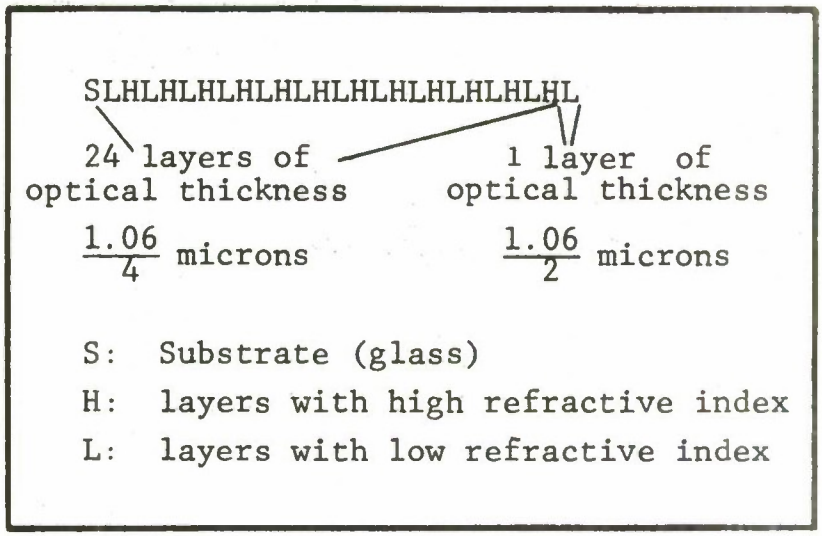

Figure 2. Optical Design of Specimen VP

The laser used for this study was a Korad K-2 multi-mode Q-switched laser with a 3/4" diameter Nd rod (see Figure 3). The maximum energy produced by this system, as measured with a Korad Calorimeter, was eight joules. The nominal half peak width of the laser pulses was 20 nsec, as measured by a Tektronix 556 oscilloscope, giving a maximum power of 400 megawatts/pulse. The irradiance (sometimes called power density) of a full power pulse averaged over its diameter was 80 megawatts/cm^2. Since this was multimode laser, the irradiance within a given pulse could vary by as much as a factor of two. For most experiments a 9 mm aperture was used in front of the sample to eliminate the less homogeneous portions of the beam.

To produce 530 nm light, 1060 nm pulses were frequency doubled with a Korad KM frequency multiplier which uses an ADP crystal. The efficiency of the crystal was such that the maximum irradiance of the 530 nm pulses was 100-150 kilowatts/cm^2.

The 1060 nm laser pulses were horizontally polarized and the 530 nm pulses were vertically polarized due to 50^o rotation of the plane of polarization within the frequency doubling crystal.

A Cary 14 spectrophotometer was used to measure transmission of the sample at low power levels and to obtain various spectral plots of the reflectors. Luminous transmittance of specimen LE was measured using a Tektronix J6503 detector (which has the same spectral response as the human eye) and an artificial daylight source (CIE standard source C) which had a color temperature of 6740^{o}K. The luminous transmittance of specimen VP was calculated from the Cary spectral plots using standard weighting factors at 100 Å intervals for the photopic observer and the CIE source C.

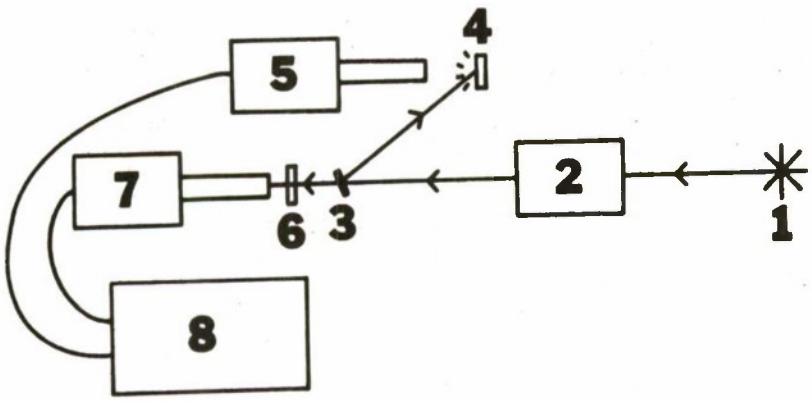

1. Laser
2. Frequency Doubler (for 530 nm pulses only)
3. Beam Splitter
4. Diffuser
5. Reference Dector
6. Sample
7. Sample Detector
8. Oscilloscope

Figure 3. Block Diagram of Experimental Apparatus

RESULTS

Part A is a presentation of the data collected from specimen LE and is followed (Part B) by the data from specimen VP. Each part is divided into 5 sections:

1. Spectral plots in the visible and near IR for various angles in each plane of polarization, and the analogous computer predictions, made as a guideline for future computer modeling;

2. Optical density vs. angle of incidence measurements, made to obtain an accurate measurement of the angular dependence of the transmission of laser radiation on angle of incidence;

3. Optical density vs. laser irradiance measurements, made to determine how reflectivity varied with power, possibly indicating damage and/or bleaching by high energy pulses;

4. Microscopic studies taken after irradiation of the dielectric coating, made to determine any slight damage not detectable by changes in optical density.

5. Luminous transmittance vs. angle measurements, taken to determine angular field effects.

Part A. Specimen LE

Transmission Spectra. Figures 4 and 5 show the comparison of the computer predicted spectral plots to the data obtained experimentally with the spectrophotometer. Vertical lines have been drawn through the plots at 530 and 1060 nm to aid in visualizing the shift in the peaks as the angle of incidence increases. Note that in both planes of polarization the optical density peaks shift toward shorter wavelengths as the angle from normal incidence increases. This shift is typical of thin film reflectors.

Optical Density vs. Angle of Incidence. These results are summarized in Figure 6. The angular dependency is not severe since the optical density remains almost constant up to about $\pm$ 35°.

Optical Density vs. Laser Irradiance. Figure 7 shows that the optical density of the specimen at 1060 nm is independent of the irradiance up to $\sim$ 70 megawatts/cm^2. This data was taken at 5° rather than normal incidence to prevent the reflected pulse from damaging the coating on the neodymium rod.

Similar plots at 530 nm would involve power densities a factor of 100 or more smaller; the films easily survive illumination at these low powers.

Microscopic Observation. Many photographs of the dielectric thin film coating were made at 100x and 250x magnification after hundreds of exposures to laser pulses. All photographs were very similar, Figure 8 being a typical example.

The hole in the upper right hand corner is just over 20μm in diameter. Bubbles and holes such as those such as those seen here were distributed uniformly over the entire surface of the reflector--apparently made during fabrication.

Although these holes are not caused by the laser, they might be significant if they allowed tiny filaments of light to pass through unattenuated or if the film were used in a converging ray region of the optical system. The filament possibility was examined by placing a piece of exposed film just behind the specimen and then exposing the specimen to several full-power pulses of the laser. The film was then examined under a microscope but no damage was observed.

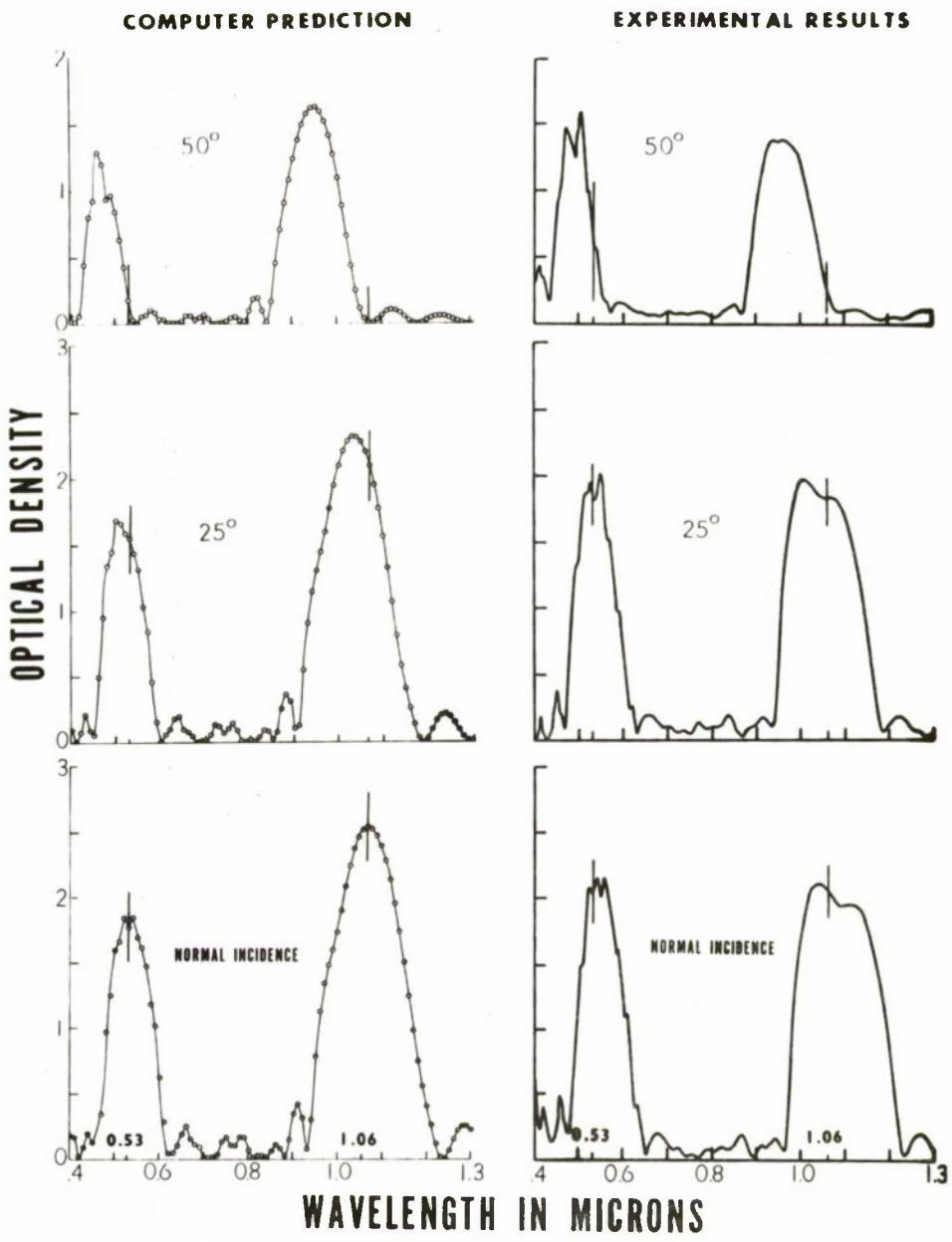

Figure 4. Optical Density vs. Wavelength for Specimen LE, for the p plane of polarization (magnetic field parallel to the film surface), for various angles of incidence, showing both computer predictions and experimental results.

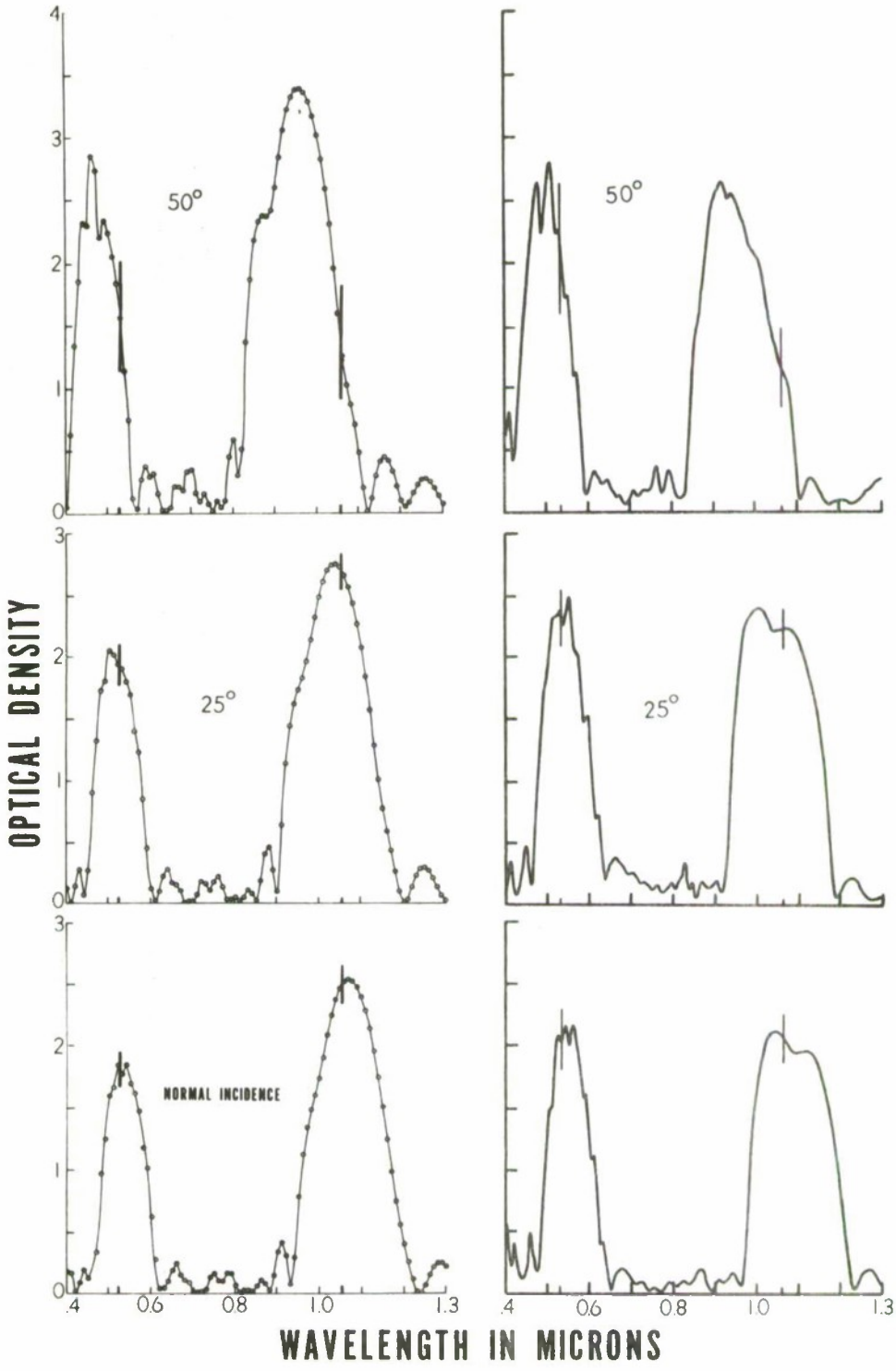

Figure 5. Optical Density vs. Wavelength for Specimen LE, for the s plane of polarization (electric field parallel to the film surface), for various angles of incidence, showing both computer predictions and experimental results.

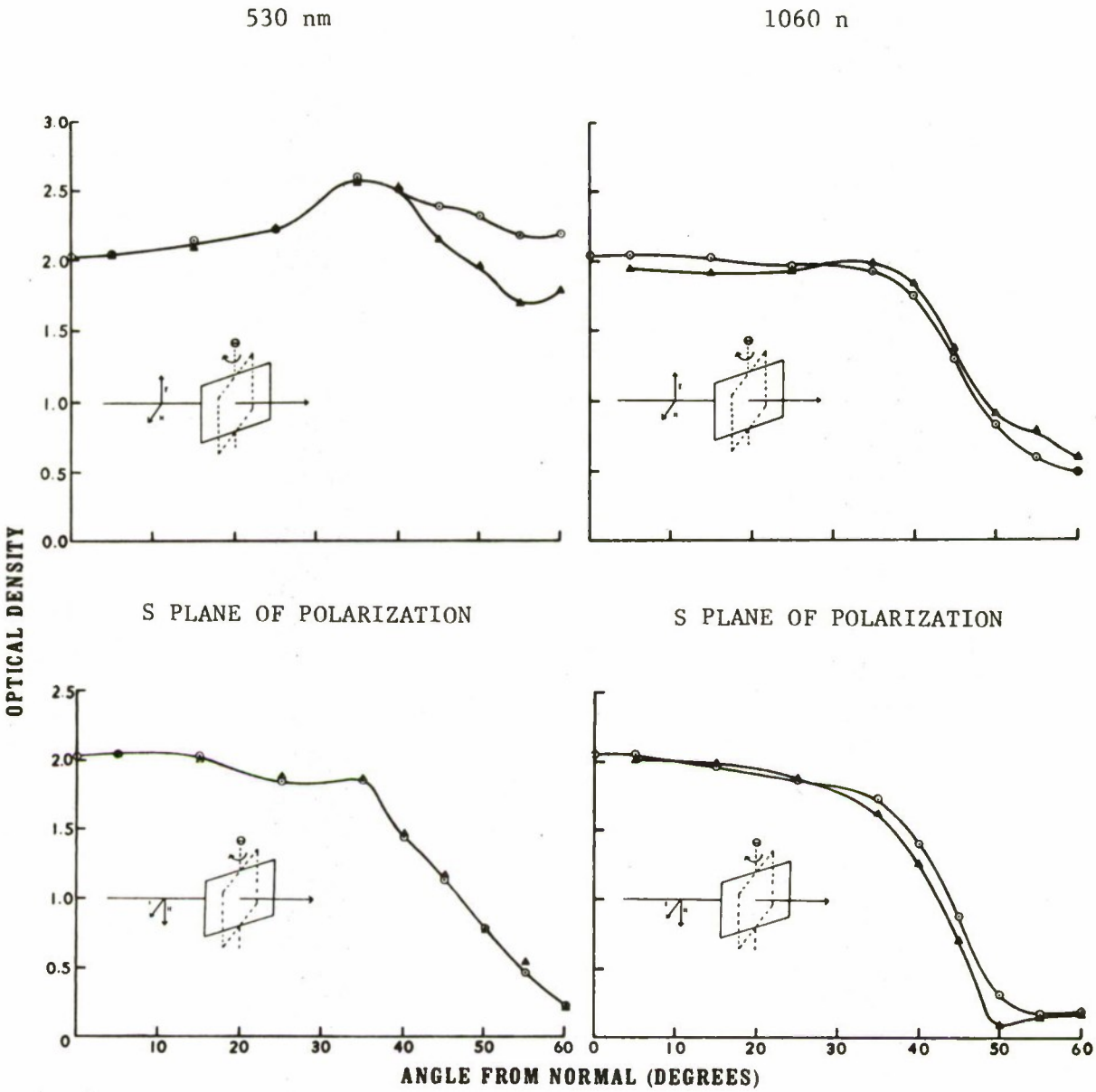

Figure 6. Optical Density vs. Angle of Incidence for Specimen LE at 530 nm (left) and 1060 nm (right), for the two planes of polarization (s at the top, p at the bottom, as measured both with the laser (data points Δ) and with the spectrometer (data points ⊙).

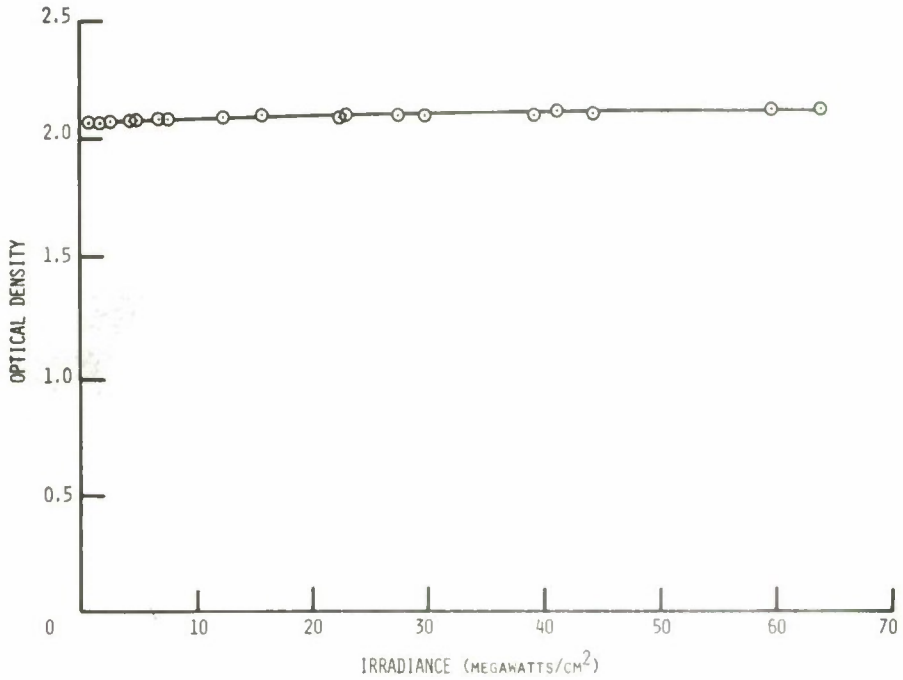

Figure 7. Optical Density vs. Irradiance for Specimen LE, at 1060 nm measured at 5^{o} from normal incidence.

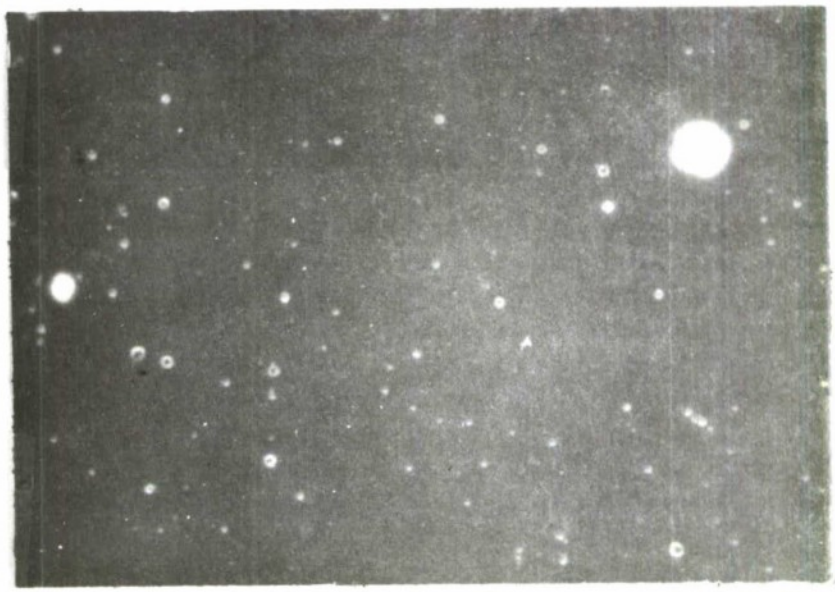

Mag: 100x

Figure 8. Photograph of the Dielectric Thin Film Coating of Specimen LE after Irradiation.

Luminous Transmittance. The results of the luminous transmittance measurements are represented in Figure 9.

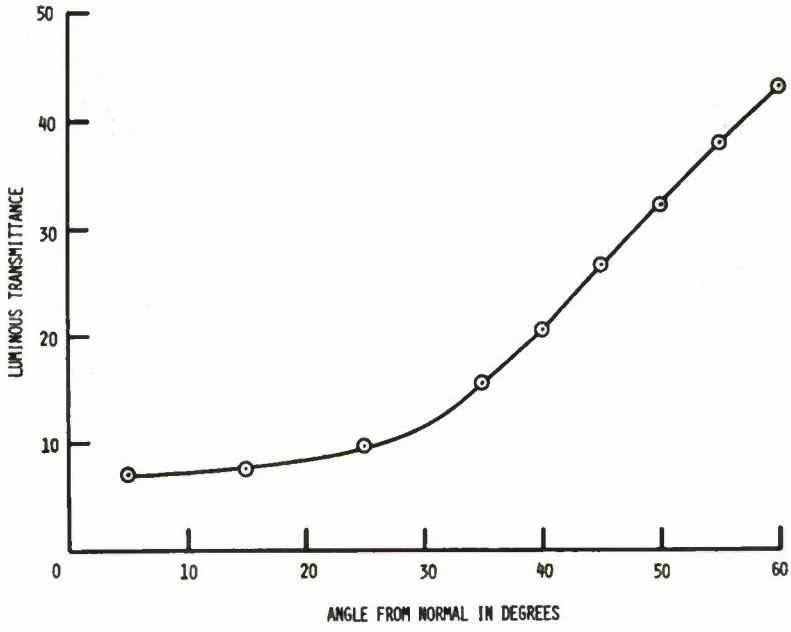

Figure 9. Luminous Transmittance vs. Angle of Incidence for Specimen LE.

Note that in the region of primary interest (angles less than 30°) the luminous transmittance is very low, less than 10 percent for this reflector. The luminous transmittance goes up with increasing angle of incidence becaust the protection at 530 nm decreases as shown on the left side of Figure 6.

Part B. Specimen VP

Transmission Spectra. Figures 10 and 11 show the theoretical and measured spectral plots for the two planes of polarization. Vertical lines indicate 1060 nm in each plot.

Optical Density vs. Angle of Incidence. The angular dependency is illustrated by the plots shown in Figure 12. Note that again the optical density remains high for $\theta \leq 30^{\circ}$.

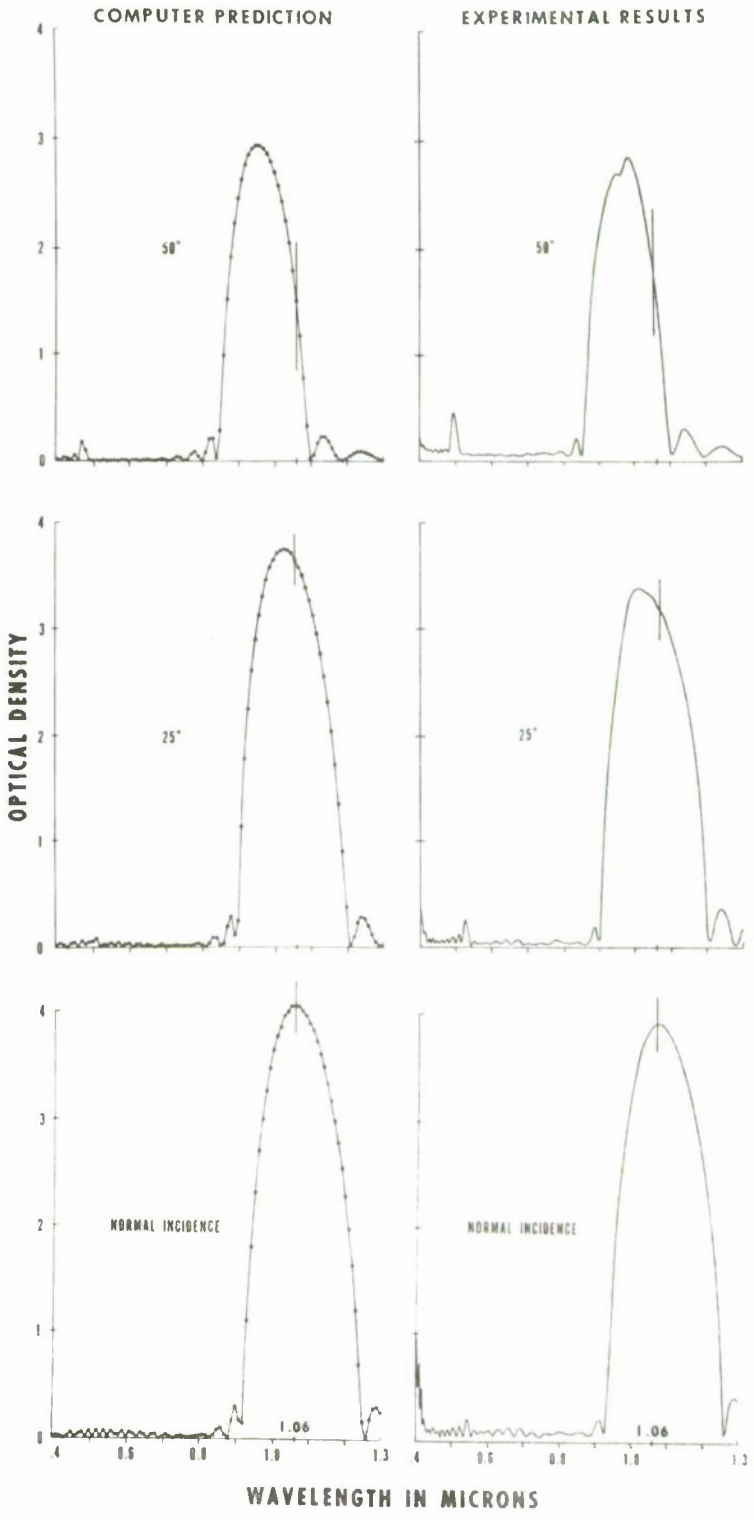

Figure 10. Optical Density vs. Wavelength for Specimen VP for the p plane of polarization (magnetic field parallel to the film surface) for various angles of incidence, showing both computer predictions and experimental results.

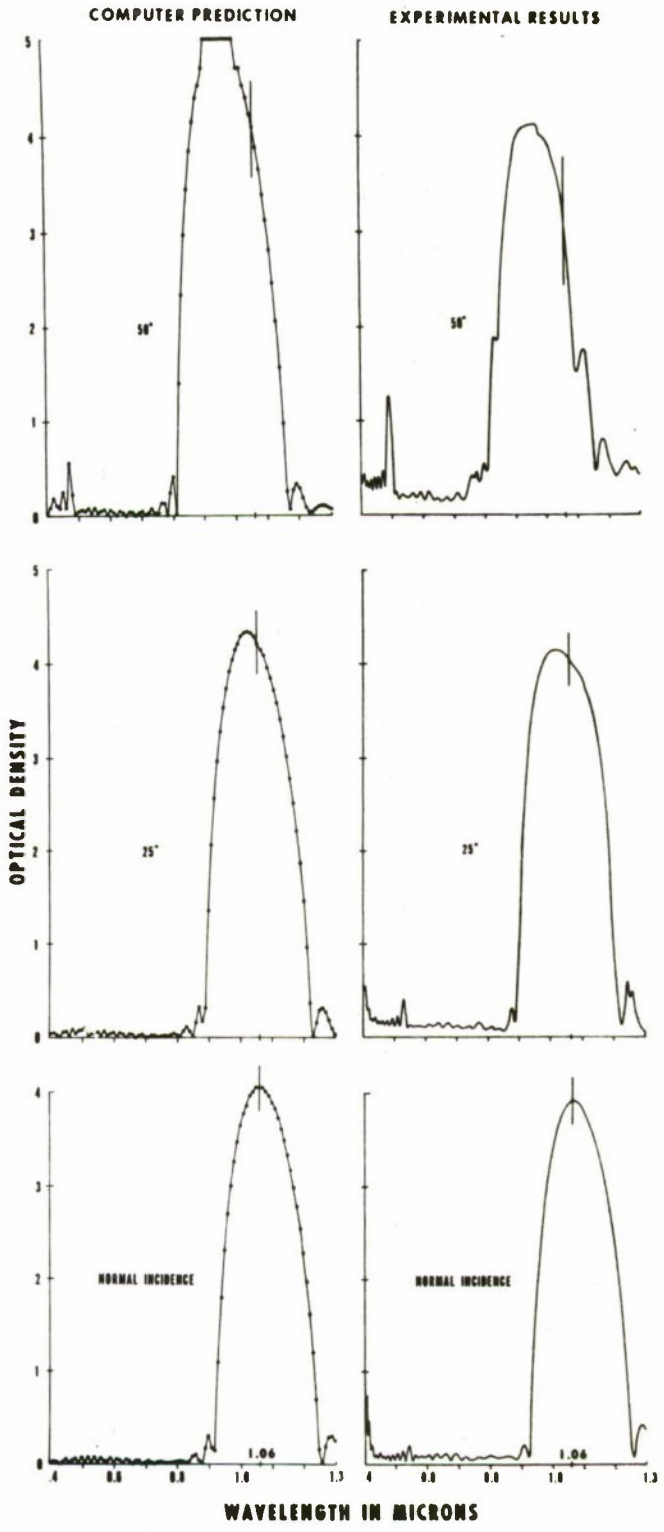

Figure 11. Optical Density vs. Wavelength for Specimen VP for the s plane of polarization (electric field parallel to the film surface) for various angles of incidence, showing both computer predictions and experimental results.

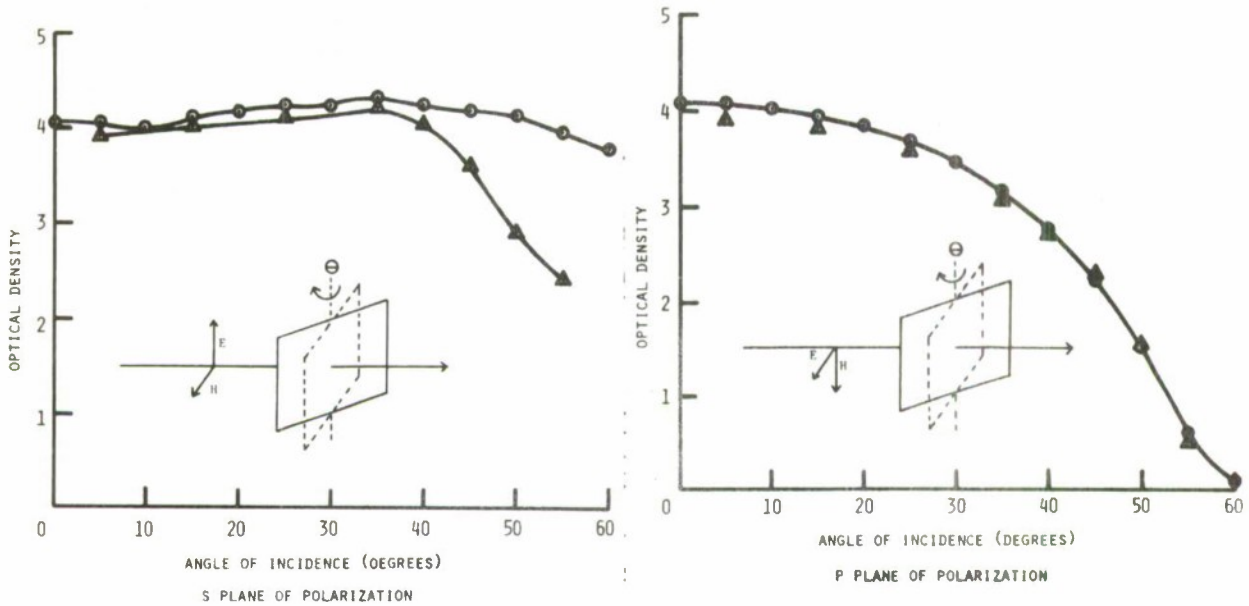

Figure 12. Optical Density vs. Angle of Incidence for Specimen VP at 1060 nm, for the two planes of polarization (s at right, p at left), as measured both with the laser (data points ▲) and with the spectrometer (data points ⊕).

Optical Density vs. Laser Irradiance. Transmission for Specimen VP is also power independent (Figure 13) indicating that the coating was able to withstand the laser pulses even up to full power of ~ 70 megawatts/cm^2.

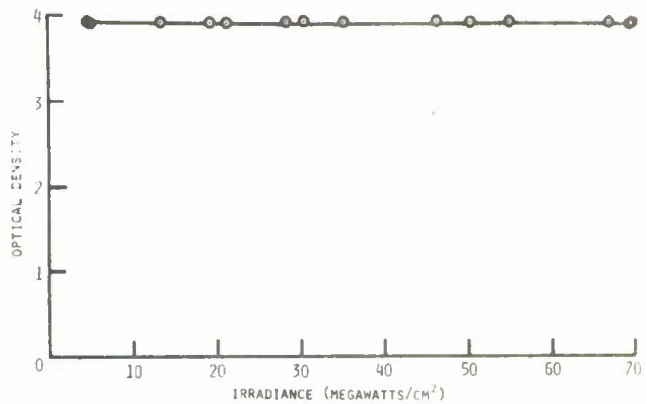

Figure 13. Optical Density vs. Irradiance for Specimen VP at 1060 nm, measured at 5° from normal incidence.

Microscopic Observation. Photographs of the portion of Specimen VP used in this study are shown in Figure 14. The origin of the irregularities apparent on the photograph is not known, but the optical density remained constant throughout the irradiation. It may indicate film fracture without removal.

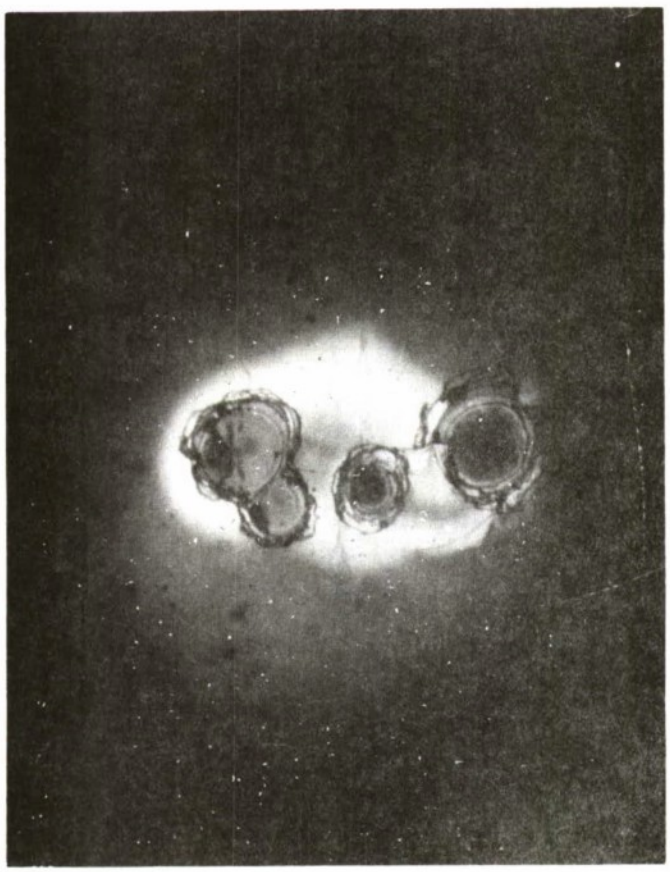

Mag: 100x

Figure 14. Photograph of the Dielectric Thin Film Coating of Specimen VP after Irradiation.

Luminous Transmitance. The luminous transmittance of Specimen VP as a function of angle of incidence is shown in Figure 15. Note that the luminous transmittance is very high, especially for small angles.

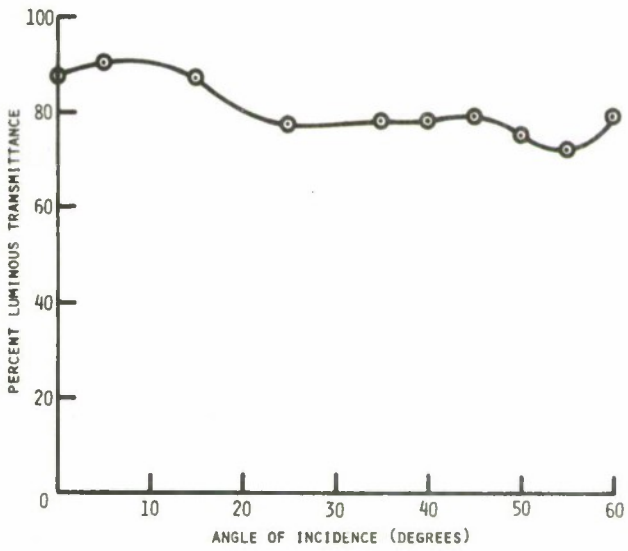

Figure 15. Luminous Transmittance vs. Angle of Incidence for Specimen VP.

DISCUSSION

There is reasonably good agreement between the experimentally obtained and theoretically calculated spectral plots shown in Figures 4, 5, 10, and 11. The discrepancies are apparently due to assumptions made when calculating the theoretical data. These include (1) that there is no absorption by the coating, (2) that there is no dispersion, and (3) that all of the layers are perfectly formed. Although each assumption probably introduces some error, it is obvious that the computer program used is very effective in predicting the major features of such reflectors.

The undulating character of the luminous transmittance vs. angle of incidence plot for Specimen VP (Figure 15) is probably an artifact due to the fact that the values of luminous transmittance for each angle were integrated numerically using weighting factors and the transmission of the specimen at various wavelengths, in increments of 100 Å throughout the visible region. Undulations reflect the unevenness of the spectral charts.

CONCLUSIONS

Sample LE

Although an optical density of two is not adequate for many applications, this specimen did show great durability. Despite the repeated handling and exposure to hundreds of laser pulses, the reflective quality of this specimen never decreased throughout the course of this study.

The sample also demonstrated a desirable insensitivity to angle of incidence. A 30° to 40° variation would be more than adequate for most applications since the acceptance half-angle of most fire control instruments is about 4°.

This sample does, however, exhibit a very low luminous transmittance (Figure 8) due to the strong reflection at 530 nm which is very nearly the center of the response curve of the human eye. Inasmuch as it may not be possible to reduce the width of that peak significantly, it would not seem feasible to use reflective coatings as a laser countermeasure for 530 nm when high visual transmittance is required unless materials and a filter design could be discovered which would allow a much narrower rejection bandwidth. On the other hand, 1060 nm radiation is far enough from the visible for reflective coatings to offer a very attractive means for protection of both the eye and optical equipment.

Sample VP

The optical density of four which was exhibited by this specimen is high enough for certain applications. If a larger optical density were required, it could be obtained by using two reflecting stacks in succession, set at a slight angle with respect to each other, or possibly even coating both sides of a fairly thick, wedge shaped substrate.

Although the specimen was undamaged during the optical density vs. irradiance measurements (Figure 13), there was an observable decrease in optical density (down to 3.5) after several dozen full power ($\geqslant 70$ MW/cm^2) laser pulses. This, however, is far more punishment than optical systems would ever be likely to receive in actual use if not placed near a focus.

Specimen VP also showed a desirable insensitivity to angle which could easily be enhanced by designing the optical stack to have a wider reflection peak, or by having the peak reflection for a wavelength slightly longer than 1060 nm. Either way, as the reflection peak moves toward shorter wavelengths with increasing angle of incidence, it would take longer for the peak to pass 1060 nm, thereby reducing the angular dependency even more. Some compromises might be needed if these filters were utilized in IR viewing systems. Excellent agreement was obtained between the computer predictions and experimental determinations of spectral transmission.

A very attractive quality of this specimen is the extremely high luminous transmittance (Figure 15). Upon visual inspection, the Valpey reflector looks like a plain piece of glass, making it very desirable as a laser countermeasure for the eye.

APPENDIX

A brief description of the basic equation used in the computer prediction of optical density vs. wavelength characteristics of thin film dielectric reflectors follows:[5]

The computer computes transmission of the reflector for a given wavelength and then converts to optical density by the equation OD = log (1/T). The equation the computer uses is abbreviated as follows:

$$T = \frac{4}{2 + A^2 \frac{n_o}{n_s} + D^2 \frac{n_s}{n_o} + \frac{C^2}{n_o n_s} + B^2 n_o n_s} \qquad (1)$$

The symbols n_o and n_s of Equation (1) refer to the refractive index of incident medium and that of the substrate. A, B, C, and D are the elements of the characteristic matrix, M,

$$M = \begin{vmatrix} A & iB \\ iC & D \end{vmatrix} \qquad (2)$$

which is a complicated matrix containing information about all layers of the thin film stack and can be used to relate the electric and magnetic fields (E and H) of the incident beam to those of the transmitted beam by the following matrix:

$$\begin{vmatrix} E \\ H \end{vmatrix} = M \begin{vmatrix} E' \\ H' \end{vmatrix} \qquad (3)$$

---

5 For more complete informatiom see the Military Standardization Handbook on Optical Design, MIL-HDBK-141, 5 October 1962, Section 20.1.5

Each layer of the reflector is characterized by a matrix of the form:

$$M = \begin{vmatrix} \cos kn_i t_i & in_i^{-1}\sin kn_i t_i \\ in_i \sin kn_i t_i & \cos kn_i t_i \end{vmatrix} \qquad (4)$$

where n_i and t_i are the refractive index and thickness of the layer, and $k = 2\pi/2$.

The characteristic matrix M of an entire system of ℓ layers is formed by taking the matrix product of the matrices from each individual layer. That is,

$$M = M_1 * M_2 * M_3 \ldots\ldots * M_\ell. \qquad (5)$$

Due to the involved nature of these parameters, Equation 1 is written in terms of A, B, C, and D as defined by Equation 2, instead of attempting to write all the terms explicitly.

Equation 1 as described above applies only to normal incidence but may be modified simply to treat non-normal incidence. In that case, the refractive index n_i must be replaced by the effective refractive index before the matrix multiplication of Equation 5 is performed to obtain the characteristic matrix M which defines the quantities A, B, C, and D of Equation 1. The refractive indices of the incident medium and of the substrate, n_o and n_s, must also be replaced by their effective values before evaluating Equation 1.

The effective refractive index is different for each of the two planes of polarization, so each plane must be evaluated separately. For the s plane of polarization (E field parallel to the film surface and perpendicular to the plane of incidence) the effective values of n_i, n_o, and n_s are $n_i\cos\theta_i$, $n_o\cos\theta$ and $n_s\cos\chi$ respectively, (See Figure 16 for the definition of angles.) For the p plane of polarization (H field parallel to film surface and perpendicular to the plane of incidence) the effective values of n_i, n_o, and n_s are $\frac{n_i}{\cos\theta}$, $\frac{n_o}{\cos\theta}$, and $\frac{n_s}{\cos\chi}$, respectively. In all cases, the values for each θ and χ are obtained from Snell's law for any given θ.

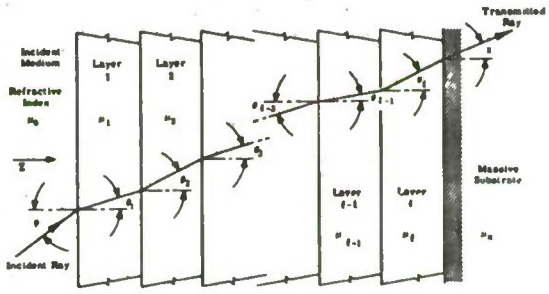

Figure 16. Nomenclature used in designating the thickness, refractive index, and angle of refraction θ in each of the layers. For sake of clarity, the reflections which take place at each interface are not shown.

REFERENCES

1. "Control of Hazards to Health from Laser Radiation," Dept. of the Army Technical Bulletin TB MED 279, 18 September 1974.

2. "E-O Sensor Susceptibility to Laser Radiation," J.R. Anderson, L. Esterowitz, and D.L. Weinberg, NRL, in The Proceedings of the 1973 DoD Laser Effects/Hardening Conference, ed. N.F. Harmon, The Mitre Corp, M73-115, April 1974, Vol. 1, p. 117; "Permament Laser Damage Thresholds of IR Detectors," L. Esterowitz, F.J. Bartoli, M.R. Kruer, and R.E. Allen, NRL Report #7867, 12 May 1975.

3. This sample was supplied by Laser Energy, Inc., Rochester, NY.

4. This sample was supplied by the Valpey Corp., Holliston, MA.

5. For more complete information see the Military Standardization Handbook on Optical Design, MIL-HDBK-141, 5 October 1962, Section 20.1.5.

DISTRIBUTION

Department of the Army
Deputy Chief of Staff for
Research, Development &
Acquisition
Washington, DC 20310

1 Attn: DAMA-ARZ,
Rm. 3E364

1 Attn: Dr. M.E. Lasser,
Chief Scientist

1 Attn: DAMA-ARZ,
Rm 3E365

1 Attn: Dr. V. Garber

1 Attn: Dr. I.R. Hershner, Jr.

1 Attn: Dr. R. Watson

1 Attn: Dr. C.H. Church

Assistant Director
Engineering Technology
Pentagon
Attn: ODDR&E, Room 3D1089
Mr. J. Persh
Washington, DC 20310

Pentagon
Attn: ODDR&E/TWP, Room 3E1025,
Dr. R.E. Schwartz
Washington, DC 20310

Headquarters, USAF
Pentagon
Attn: AF/RDPA, Room 5D332,
LTC Guest
Washington, DC 20310

Commander
US Army Foreign Science &
Technology Center
Federal Office Bldg.
Charlottesville, VA 22901

Commander
US Army Materiel, Development and
Readiness Command
5001 Eisenhower Avenue
Alexandria, VA 22333

1 Attn: AMCDL,
Mr. N. Klein

1 Attn: DRCDE,
BG H. Griffith

1 Attn: DRCDE-PE,
Mr. T. Jasczcult

1 Attn: DRCDE-TP,
Mr. P. Chernoff

1 Attn: DRCSA-BC,
Mr. Z. Tashjian

1 Attn: DRCDE-MT,
Mr. E. Sedlak

1 Attn: DRCDE-TC,
Mr. R. Zentner

Commander
US Army Armament Command
Rock Island, IL 61201

1 Attn: DRSAR-RD-CG,
MG J. Raaen

1 Attn: DRSAR-RD,
Mr. J. Brinkman

1 Attn: DRSAR-RDT,
Mr. J. Turkeltaub

1 Attn: DRSAR-RDT,
Dr. R.L. Moore

1 Attn: DRSAR-RDM,
Mr. R. Chandler

1 Attn: DRSAR-RDC,
Mr. E. Vaughan

DISTRIBUTION (Cont'd)

Commander
Aberdeen Proving Ground
Aberdeen, MD 21005

1 Attn: AMSTE-SA-E,
Mr. J. Bialo

1 Attn: AMSTE-ME,
Mr. J. Steedman

1 Attn: AMXBR-TD,
Dr. R. Eichelberger

1 Attn: AMXSY-D,
Dr. J. Sperrazza

1 Attn: AMXSY-GS,
Mr. C. Odom

Commander
US Army Missile Command
Redstone Arsenal, AL 35809

1 Attn: AMSMI-RR,
Dr. G. Miller

1 Attn: AMSMI-R,
MAJ M. O'Neill

1 Attn: AMSMI-R,
Dr. J. McDaniel

1 Attn: AMSMI-REI,
Mr. John Asbell

1 Attn: AMSMI-RFGA,
Mr. Fowler

1 Attn: AMSMI-R,
Dr. R. Conrad

Commander
US Army Electronic Proving Ground
Attn: STEEP-T-B1
Fort Huachuca, AZ 85613

Commander
US Army Electronics Command
Fort Monmouth, NJ 07703

1 Attn: AMSEL-CT-L,
Mr. B. Louis

1 Attn: AMSEL-CT-L,
Dr. R. Buser

1 Attn: AMSEL-CT-L,
Mr. V. DeMonte

1 Attn: AMSEL-CT-L,
Mr. M. Mirachi

Commander
US Army Dugway Proving Ground
Attn: TL, Technical Library
Dugway, UT 84022

Commander
US Army Research Office-Durham
Box CM, Duke Station
Attn: Dr. R.J. Lontz
Durham, NC 27706

Commander
US Army Natick Research & Development
Command
Attn: AMXRE-PRD, Dr. E. Healy
Natick. MA 01760

Commander
Attn: MASSTER,
MG S. Meyer
Fort Hood, TX 76544

Commander
Harry Diamond Laboratories
2800 Powder Mill Road
Adelphi, MD 20783

1 Attn: AMXDO-RCB,
Dr. H. Gibson

1 Attn: AMXDO-RCB,
Dr. T. Gleason

DISTRIBUTION (Cont'd)

Commander
White Sands Missile Range
White Sands, NM 88002

1 Attn: AMSEL-WL-ML,
Mr. J. Bert

1 Attn: STEWS-ID-A,
Mr. G. Galos

Commander
Yuma Proving Ground
Attn: STEYP-AD, Technical Library
Yuma, AZ 85364

Commander
Naval Research Laboratory
Washington, DC 20390

1 Attn: Dr. R. Andersen,
255 Bldg. 58

1 Attn: Dr. A. Schindler,
200 Bldg. 42

Commander
Air Force Armament Laboratories
Attn: DLOS
Eglin AFB, FL 32542

Commander
Rocky Mountain Arsenal
Attn: SARRM-CS, Dr. W. McNeill,
Chief Scientist
Denver, CO 80240

Department of the Air Force
Air Force Avionics Laboratory
(AFSC)
Wright Patterson AFB, OH 45433

1 Attn: Mr. R. Firsdon

1 Attn: ASD/RWT

President
US Army Armor & Engineering Board
Attn: STEBB-CV
Fort Knox, KY 40121

Air Force Weapons Laboratory
Kirtland Air Force Base
Attn: CPT M. Kemp, Bldg. 497
Albuquerque, NM 87116

Director Electronic Warfare
Electronic Warfare Laboratory
Fort Monmouth, NJ 07703

1 Attn: AMSEL-WL-D,
Mr. J. Charlton

1 Attn: AMSEL-WL-D,
Mr. C. Hardin

Advanced Research Projects Agency
Architect Bldg.
Attn: Dr. P. Clark
1400 Wilson Blvd.
Arlington, VA 22209

Advisory Group on Electron Devices
Attn: Secretary, Working Group on
Lasers
201 Varick St.
New York, NY 10014

COL Richard McLean
Weapons System Evaluation Group
400 Army/Navy Drive
Arlington, VA 22202

Dr. M.P. Pastel
Scientific Advisor--TRADOC
Attn: ATDC-SI
Fort Monroe, VA 23651

Mr. Everett Richey
School of Aerospace Medicine
Brooks Air Force Base
San Antonio, TX 78235

Defense Documentation Center (12)
Cameron Station
Alexandria, VA 22314

Printing & Reproduction Division
FRANKFORD ARSENAL
Date Printed: 14 May 1976

DISTRIBUTION (Cont'd)

Commander
Frankford Arsenal
Philadelphia, PA 19137

1 Attn: SARFA-AOA-M

1 Attn: SARFA-TD

1 Attn: SARFA-PD

1 Attn: SARFA-PDR

6 Attn: SARFA-PDS

1 Attn: SARFA-PDC

1 Attn: SARFA-FC

1 Attn: SARFA-FCD-O

1 Attn: SARFA-QA

1 Attn: SARFA-FI

1 Attn: SARFA-PA

3 Attn: SARPA-TSP-L/51-2
1 - Reference Copy
1 - Circulation Copy
1 - Tech Reports Editing Br.

Printing & Reproduction Division
FRANKFORD ARSENAL
Date Printed: 14 May 1976